ORIGINAL PAPER

Evaluation of Strength and Deformability of Soft Sedimentary Rocks in Dry and Saturated Conditions Through Needle Penetration and Point Load Tests: A Comparative Study

Á. Rabat[1] · M. Cano[1] · R. Tomás[1] · Á. E. Tamayo[1] · L. R. Alejano[2]

Abstract

The preparation of standardized soft rock specimens to perform unconfined compressive strength (UCS) tests is typically difficult, expensive and time-consuming. Needle penetration test (NPT) was originally developed in Japan as an alternative for the indirect estimation of UCS of soft rocks. The needle penetrometer is a simple, portable and non-destructive testing device that measures applied load and penetration depth for the rock to calculate the needle penetration index (NPI). A complimentary, portable and widely used destructive test is the point load test (PLT), which measures regular and irregular specimens by the application of a concentrated load using two coaxial conical platens that yield the point load strength index ($I_{S(50)}$). We investigated and compared the NPT and PLT in terms of measuring changes induced by water saturation and obtaining UCS and the static Young's modulus (E_{st}) for dry and saturated soft sedimentary rocks. The results point to significant correlation functions from which to infer UCS and E_{st} in terms of NPI and $I_{S(50)}$ in dry and saturated soft rocks. Furthermore, both NPT and PLT are suitable tests for evaluating changes in strength and deformability induced by water saturation. We also found a good correlation between the NPI and $I_{s(50)}$.

List of Symbols

E_{st}	Static Young's modulus
$I_{s(50)}$	Point load strength index
k	Ratio between UCS and $I_{s(50)}$
F	Applied load in the NPT
D	Penetration depth in the NPT
ρ_d	Dry density
ρ_{sat}	Saturated density
p_o	Open porosity
p	Total porosity
W_a	Water absorption
χ	Mean value
σ	Standard deviation
R	Coefficient of correlation
R^2	Coefficient of determination

Abbreviations

FLD	Field
LAB	Laboratory
NPI	Needle penetration index
NPT	Needle penetration test
PLT	Point load test
UCS	Unconfined compressive strength

✉ Á. Rabat
alvaro.rabat@ua.es

1 Department of Civil Engineering, University of Alicante, Carr. San Vicente del Raspeig, 03690 San Vicente del Raspeig, Alicante, Spain

2 Department of Natural Resources and Environmental Engineering, University of Vigo, Campus Universitario Lagoas-Marcosende, s/n, 36310 Vigo, Spain

1 Introduction

Unconfined compressive strength (UCS) is an essential geomechanical property for rock mass characterization, description and classification, widely used in mining, civil engineering, geotechnical and infrastructure projects. While the test procedure itself is relatively simple, UCS determination is expensive and time-consuming because of the need to use heavy test equipment and well-prepared standard specimens. Furthermore, for certain rock types, e.g., argillaceous and very soft rock, it is especially complicated to

prepare specimens of the size and shape necessary to carry out strength and deformability tests (Li et al. 2016).

For those reasons, UCS has traditionally been indirectly assessed using alternative methods like the point load test (PLT) and Schmidt hammer test. The PLT can be conducted using irregularly shaped specimens, thereby eliminating the need to use heavy laboratory equipment, but the drawback is that it is difficult to obtain a unique accurate value for the k factor correlating the point load strength index ($I_{S(50)}$) and UCS (i.e. $k = UCS/I_{S(50)}$), given the strong effects of weathering degree and rock type (Ulusay and Erguler 2012). As for the Schmidt hammer test, this can be used to estimate the UCS in-field geotechnical surveys but has two drawbacks, namely, that it is not suitable for rocks with UCS values lower than 10 MPa (Ulusay and Erguler 2012) and it cannot be applied in a non-destructive manner in soft rocks, given that high-energy impacts can cause microcracking, grain crushing and pore collapse in friable, porous or weathered rock specimens (Aydin 2009). Those tests, therefore, are not suitable for in situ non-destructive tests to determine mechanical properties in natural soft rock structures, monuments or heritage or ancient constructions built with natural stone (Ulusay et al. 2014).

With the aim of overcoming the above-mentioned limitations, a needle penetrometer was developed by the Rock Mechanics Committee of the Japan Society of Civil Engineers (JSCE-RMC) as a portable and non-destructive testing device for soft rock specimens. NPT is similar to the Cone Indention Test developed at the National Coal Board of England to determine both the Indentation Hardness Index (IHI) and UCS of rock (Szwedzicki 1998; Tiryaki and Bolukbasi 2007). In this sense, Kahraman and Gunaydin (2008) obtained that IHI can be used for predicting the sawability of carbonate rocks and Kahraman et al. (2012) suggested correlation functions to indirectly predict the UCS and the Brazilian Tensile Strength (BTS) from the IHI. In this connection, NPT could be also used for the determination of the specific energy of cutting or for the indirect determination of strength parameters of soft rocks, such as the UCS. This approach, especially suitable for testing specimens with UCS values lower than 20 MPa, has three major advantages: NPT can be used in the field or laboratory, the specimens do not require any special preparation, and it is non-destructive (Ulusay et al. 2014). The NPI has been mostly used to calculate the UCS of sedimentary soft rocks (like marls, shales, sandstones and argillaceous rocks) in a dry state in laboratory tests or with their natural water content in field surveys. However, very little research has focused on NPI estimates for fully water-saturated specimens or on the NPI relationships with both the static Young's modulus (E_{st}) and the $I_{S(50)}$.

Our study tries to close all those gaps. Specifically, our main objectives were: (a) to evaluate the changes induced by water saturation of siltstone and gypsiferous rock using the NPT and PLT; (b) to verify the suitability of the NPT and PLT to indirectly obtain the UCS and E_{st} of siltstone and gypsiferous rock in dry and saturated water conditions; and (c) to evaluate significant relationships between the $I_{S(50)}$ and the NPI.

2 Previous Studies

A seminal study on the relationship between the NPI and UCS was conducted by Ulusay and Erguler (2012), who developed a database consisting of more than 700 NPI-UCS data pairs for different rock types (marl, siltstone, mudstone, sandstone, greywacke, tuff and shale), obtained from both previous publications and their own tests. Those authors suggested the following correlation function:

$$UCS = 0.4 \cdot NPI^{0.929} \tag{1}$$

where UCS is measured in MPa and the NPI in N/mm.

Although the correlation proposed by those authors is a power function, Aydan (2012) subsequently found the following linear relationship between both parameters for numerous rock types (tuff, sandstone, pumice, limestone, lignite, mudstone, siltstone, marl and loam):

$$UCS = 0.2 \cdot NPI \tag{2}$$

where UCS is measured in MPa and the NPI in N/mm.

Aydan (2012) suggested that correlation would be improved if the fitting function was obtained individually for each rock type, further indicating that the conversion factor usually takes a value between 0.06 and 0.70.

Aydan and Ulusay (2013) subsequently obtained the following linear correlation for Turkish tuff:

$$UCS = 0.3 \cdot NPI \tag{3}$$

where UCS is measured in MPa and the NPI in N/mm.

Others authors have found significant relationships between the NPI and UCS for several natural soft rock types (Okada et al. 1985; Yamaguchi et al. 1997; Takahashi et al. 1998; Naoto et al. 2004; Uchida et al. 2004; Kahraman et al. 2017). Furthermore, the NPT is now widely implemented in Japan to check the quality and estimate UCS for soilcrete columns using the high-pressure chemical churning pile (jet grouting) method originally devised by Ichise et al. (1974).

Most of the correlations proposed in the literature, compiled in Table 1, are linear or power functions. Regarding the relationship between E_{st} and the NPI, Aydan (2012) found a linear correlation between both parameters for tuffs, lignites, sandstones and limestones, suggesting that the conversion factor usually varies between 0.015 and 0.120. Aydan and

Table 1 Equations correlating unconfined compressive strength (UCS) or static Young's modulus (E_{st}) with the needle penetration index (NPI) found in previous studies

Authors	Correlation function	Measurement units		Rock types
		UCS or E_{st}	NPI	
Okada et al. (1985)	$\log UCS = 0.978 \cdot \log NPI + 1.599$ ($R = 0.914$) (4)	kg/cm^2	kg/mm	Rocks and soilcrete
Yamaguchi et al. (1997)	$\log UCS = 0.982 \cdot \log NPI - 0.209$ ($R = 0.872$) (5)	kg/cm^2	kg/cm	Pyroclastic rocks
Takahashi et al. (1998)	$UCS = 1.5395 \cdot NPI^{0.9896}$ ($R = 0.90$) (6)	MPa	N/mm	Sandstone, siltstone, conglomerate, greywacke, volcanic tuff
Naoto et al. (2004)	$UCS = 41.8 \cdot NPI - 4$ ($R = 0.899$) (7)	kN/m^2	N/cm	Hard claystone
Uchida et al. (2004)	$UCS = 27.3 \cdot NPI + 132$ (8)	kPa	N/cm	Sandstone
Erguler and Ulusay (2007, 2009)	$UCS = 0.51 \cdot NPI^{0.8575}$ ($R = 0.87$) (9)	MPa	N/mm	Marble, siltstone, shale, tuff
Ulusay and Erguler (2012)	$UCS = 0.402 \cdot NPI^{0.929}$ ($R = 0.89$) (10)	MPa	N/mm	Marl, tuff, shale, siltstone, sandstone, greywacke, mudstone
Aydan (2012)	$UCS = 0.2 \cdot NPI$ (11)	MPa	N/mm	Tuff, sandstone, pumice, limestone, lignite, mudstone, siltstone, marl, loam
	$E_{st} = 0.12 \cdot NPI$ (Upper limit) (12.a) $E_{st} = 0.05 \cdot NPI$ (12.b) $E_{st} = 0.015 \cdot NPI$ (Lower limit) (12.c)	GPa	N/mm	
Aydan and Ulusay (2013)	$UCS = 0.3 \cdot NPI$ (13)	MPa	N/mm	Turkish tuffs
	$E_{st} = 25 \cdot NPI$ (14)	MPa	N/mm	
Kahraman et al. (2017)	$UCS = 0.35 \cdot NPI$ (15)	MPa	N/mm	Cayirham coal

Ulusay (2013) also found a linear correlation for tuffs in the Cappadocia region of Turkey (Table 1).

Changes in the NPI produced by water content remains under-researched, with just a few papers published on this subject (Aydan 2012; Ulusay et al. 2014). Those works, which studied the relationship between saturation and the NPI for Japanese, Turkish and Egyptian soft rocks, concluded that the NPI decreases as rock water content increases, as also do UCS and E_{st}. The same authors also analysed NPI variations in line with the number of drying-wetting and thawing-freezing cycles, suggesting the possibility of using the needle penetrometer to assess rock degradation or weathering.

The PLT, in contrast, has been extensively studied, with hundreds of correlations proposed for the $I_{S(50)}$ with the UCS. However, the number of studies of soft rocks such as siltstones and gypsiferous rocks is small. Although the International Society for Rock Mechanics (ISRM) (Franklin 1985) established that the UCS/$I_{s(50)}$ ratio could vary from 15 to 50 due to anisotropy and the large variety of rocks, this ratio could be lower than 15 for siltstones and gypsiferous rocks. Along those lines, Smith (1997) determined that the UCS/$I_{s(50)}$ ratio ranged from 8 to 15 for weak rock materials from coastal US deposits, while Sadeghiamirshahidi and Vitton (2019) suggested 6.6 to 7.7 for Michigan Basin gypsum. A summary of the UCS/$I_{s(50)}$ ratios found in the literature for different sedimentary and soft rocks is given in Table 2.

Furthermore, very few papers have focused on the indirect determination of E_{st} using the $I_{s(50)}$; one was the noteworthy laboratory work carried out by Daoud et al. (2017) on Iraqi limestones and sandstones, for which a power function correlation between both parameters was determined. Another relatively unexplored topic is PLT evaluation of changes in rock properties caused by water saturation. Khono and Maeda (2012) found reductions of 15–98% in the $I_{s(50)}$ and 18.5–97.1% in UCS for several types of volcaniclastic rocks, Kahraman (2014) reported reductions of up to 37.8% in the $I_{s(50)}$ and 40.4% in UCS for pyroclastic rocks, while Sadeghiamirshahidi and Vitton (2019) measured decreases of 53.6% in the $I_{s(50)}$, 41.1% in UCS and 49.6% in the E_{st} for Michigan Basin gypsum.

We attempt to go beyond the scope of previous investigations in our comparative study of the applicability of NPT and PLT to estimates of the strength and deformability of dry and saturated soft sedimentary rocks from southeastern Spain.

3 Methodology

3.1 Rock Block Collection and Specimen Preparation

Two different lithologies widely present in the province of Alicante (Spain) were studied for this research: a Neogene

Table 2 Unconfined compressive strength (UCS) and point load strength index ($I_{s(50)}$) ratios for sedimentary and soft rocks reported in previous studies

Authors	$K = UCS/I_{s(50)}$	Rock type
Broch and Franklin (1972)	24	Several rock types (mainly sandstones)
Bieniawski (1975)	23	Sandstone (South Africa)
Carter and Sneddon (1977)	21–22	Coal measures (UK)
Al-Jassar and Hawkings (1979)	17–30	Carboniferous limestones (UK)
Read et al. (1980)	16	Several sedimentary rocks (Australia)
ISRM and Franklin (1985)	20–25	Several rock types
Das (1985)	14.7–18	Siltstone and sandstone (Canada)
Vallejo et al. (1989)	12.5–17.4	Sandstone and shale (USA)
Jermy and Bell (1991)	14.1	Coal measures (South Africa)
Smith (1997)	8–15	Harbour dredge materials
Hawkins (1998)	7–68	Sandstones, limestones and chalks (UK)
Rusnak and Mark (2000)	19.6–22.4	Shale, siltstone, sandstone and limestone (USA)
Tsiambaos and Sabatakakis (2004)	23	Limestone, marlstone and sandstone (Greece)
Palchik and Hatzor (2004)	8–18	Porous chalks
Sabatakakis et al. (2008)	13–28	Marlstones, sandstones and limestones
Diamantis et al. (2009)	19.8	Serpentinites (Greece)
Tziallas et al. (2009)	14.5	Sedimentary and metamorphic rocks (Greece)
Singh et al. (2012)	21–23	Harder rocks (sandstone, limestone, dolomite)
	14–16	Softer rocks (Khondalite, shale, rock salt)
Kohno and Maeda (2012)	16.4	Volcaniclastic rocks (Japan)
Li and Wong (2013)	19.8–21.3	Meta-siltstone and meta-sandstone (Singapore)
Kahraman (2014)	8.7	Pyroclastic rocks (Turkey)
Sadeghiamirshahidi and Vitton (2019)	6.6–7.7	Michigan Basin gypsum

siltstone collected from an outcrop located in the peri-urban area of Alicante city and a Keuper Triassic gypsiferous rock extracted from an outcrop in the municipality of Finestrat (Fig. 1). For the siltstone, four homogeneous rock blocks (labelled S1 to S4) were carefully selected and visually inspected to ensure the absence of fractures, joints and areas with different degrees of weathering. For the gypsiferous rock, five blocks (labelled G1 to G5) were also meticulously selected but showing, in this case, important weathering and an intrinsic heterogeneity due to the presence of red and green clayey clasts. Also identified in the gypsiferous blocks were some Jacinto quartzes (smaller than 1 cm).

Each of the nine blocks was large enough to extract the specimens necessary to carry out all mechanical test types (Fig. 1). To carry out the NPT according to the ISRM-suggested method (Ulusay et al. 2014), from each block, four cylindrical core specimens, 52 mm in diameter and 50–55 mm in length, were drilled perpendicular to bedding using a diamond drill rig. Additionally, to carry out the PLT, drilled from each block was a minimum of sixteen cylindrical core specimens, 28 mm in diameter and 70–75 mm in length. Finally, to calculate UCS and E_{st}, drilled from each block was a minimum of eight cylindrical core specimens, 28 mm in diameter and 70–75 mm in length to ensure a minimum slenderness (diameter:length) ratio of 2.5 for the UCS test, as required by various standards (ISRM 1977; AENOR 1990a).

To prepare dry and fully saturated specimens for each block/test and achieve the necessary constant final mass, half of the specimens were dried in an oven at 50 °C and the other half were soaked in water in a vacuum chamber. That is, at certain time intervals, the specimens were removed from the oven or the saturation chamber, weighed and immediately reintroduced in them until a constant mass was reached. Specifically, the immersion time necessary for full water saturation was less than 48 h in this type of rocks.

3.2 Test Procedures

3.2.1 Chemical and Mineralogical Analyses

To study how chemical and mineral composition and water saturation weakened the strength of the selected rocks, we performed the following analyses: thin-section petrographic analysis, using an OPTIKA B600POL petrographic microscope with the X4 objective lens; carbonate content determination, using a Bernard calcimeter according to UNE 103-200-93 (AENOR 1993); X-ray fluorescence (XRF), conducted using a PHILIPS MAGIX PRO X-ray sequential spectrometer equipped with a rhodium X-ray tube and beryllium window and a single goniometer-based
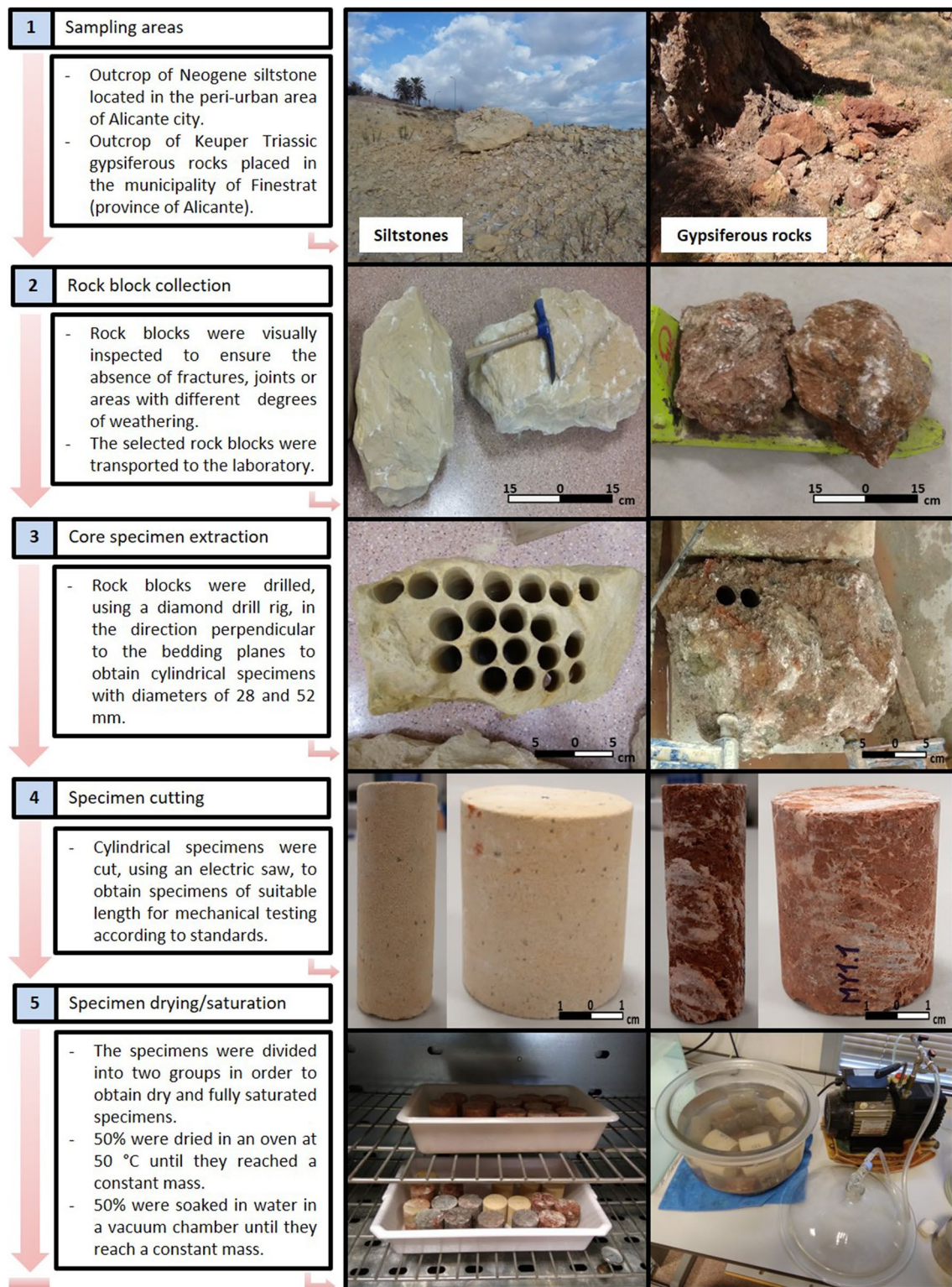
Fig. 1 Rock block collection and specimen preparation

measuring channel covering the complete measurement range, according to ASTM E1621-13 (E1621-13, 2013); and, finally, X-ray diffraction (XRD), conducted using a Bruker D8-Advance X-Ray diffractometer with a KRISTAL-LOFLEX K 760-80F X-ray generator and XR tube with a copper anode.

3.2.2 Physical Properties

Dry and saturated bulk densities (ρ_d and ρ_{sat}) were calculated, according to UNE-EN 1936 (AENOR 2007), by dividing the specimen's dry or saturated weight by the specimen's bulk volume, calculated from diameter and length measured using a Vernier caliper. True density (ρ_r) was determined using the pycnometer method in accordance with UNE 103-302-94 (AENOR 1994).

Open porosity (p_o) was measured using specimen dry, submerged and saturated weights and specimen volume according to UNE-EN 1936 (AENOR 2007). Total porosity (p) was computed from rock dry density and true density (AENOR 2007). Water absorption (W_a) was calculated as the ratio between the saturated mass after immersion for 48 h and the dry mass of the specimens, according to UNE-EN 13755 (AENOR 2008).

Pore-size distribution and, hence, rock porosity, was measured using the mercury intrusion porosimetry (MIP) technique: one MIP test for the siltstone and 3 MIP tests for the gypsiferous rock (due to its greater heterogeneity).

3.2.3 Mechanical Properties

A servo-controlled press with a capacity of 200 kN (MUF-401 Servosis) was used to carry out the strength and deformability tests. Specimen strain was measured using a specific instrument consisting of two joined metal rings positioned in parallel along the specimen axis and two diametrically opposed linear variable differential transducers that recorded changes in the axial relative distance between rings during unloading–reloading cycles. Axial strain was measured up to a maximum value equal to 50% of the failure load of specimens to obtain the secant E_{st} according to UNE 22950-3 (AENOR 1990b). Once the deformability test was concluded, the rings were removed from the specimen and the loading tests were repeated until failure. The loading rate was adjusted to make sure that specimen failure in dry and saturated states happened between 5 and 10 min after starting the test, as required by UNE 22950-1 (AENOR 1990a).

The PLT was performed using a digital device (45-D0550 Controls) that diametrically tested the core specimens. Size correction was applied to calculate the $I_{s(50)}$ in accordance with the ISRM standard (Franklin 1985).

Fig. 2 **a** Needle penetration test (NPT). **b** Needle penetrometer used in this work. **c**, **d** Dry and saturated siltstone specimens, respectively, after NPT. **e**, **f** Dry and saturated gypsiferous rock specimens, respectively, after NPT. The circles indicate the points where testing was done
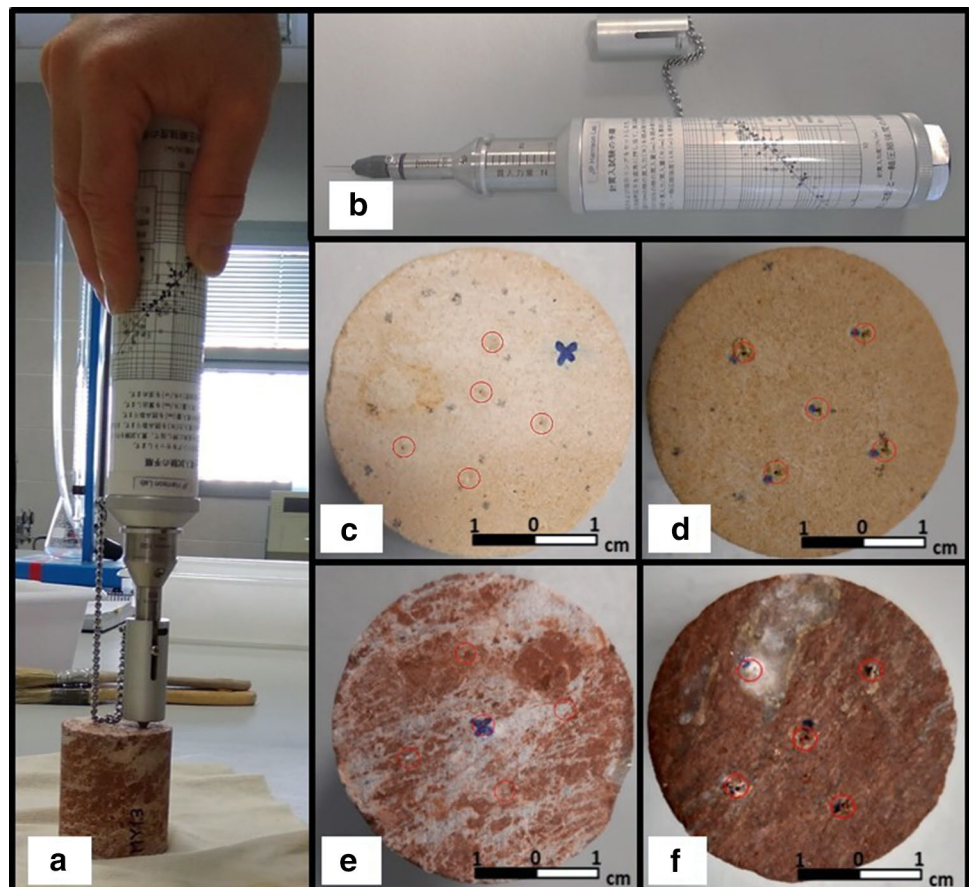
The NPT, using the device developed by Maruto Co. ([2006](#)), was performed five times for each specimen surface, under the premise that each penetration point was at least 10 mm from any other point, according to the ISRM (Ulusay et al. [2014](#)) (Fig. [2](#)). The NPI was then calculated as follows:

$$\text{For } F = 100N \text{ and } D \le 10 \text{ mm,} \quad \text{NPI} = \frac{100}{D} \tag{16.a}$$

$$\text{For } D = 10 \text{ mm and } F < 100N, \quad \text{NPI} = \frac{F}{10} \tag{16.b}$$

where F is the applied load (in N) and D is the penetration depth (in mm).

4 Results

4.1 Chemical and Mineralogical Composition

XRF analyses showed that the main chemical compounds in the siltstone were CaO (44%) and SiO_2 (8%), with loss on ignition (LOI) of 44%, while the main chemical compounds in gypsiferous rock were SO_3 (36–42%), CaO (27–35%), SiO_2 (7–8%) and MgO (3–7%), with LOI of 3–20% (Table [3](#)). XRD revealed that calcite and quartz were the main minerals in the siltstone, while gypsum, bassanite, dolomite and quartz were the dominant minerals in the gypsiferous rock (Fig. [3](#)). Small amounts of clay (aluminosilicates) were also found in both lithologies.

In line with above-mentioned results, Bernard calcimeter tests revealed that carbonate content was 92–94% for the siltstone and 1–4% for the gypsiferous rock.

Table 3 Chemical composition (% oxides) for siltstone (S2) and gypsiferous rock (G1, G3 and G5) obtained by XRF analyses
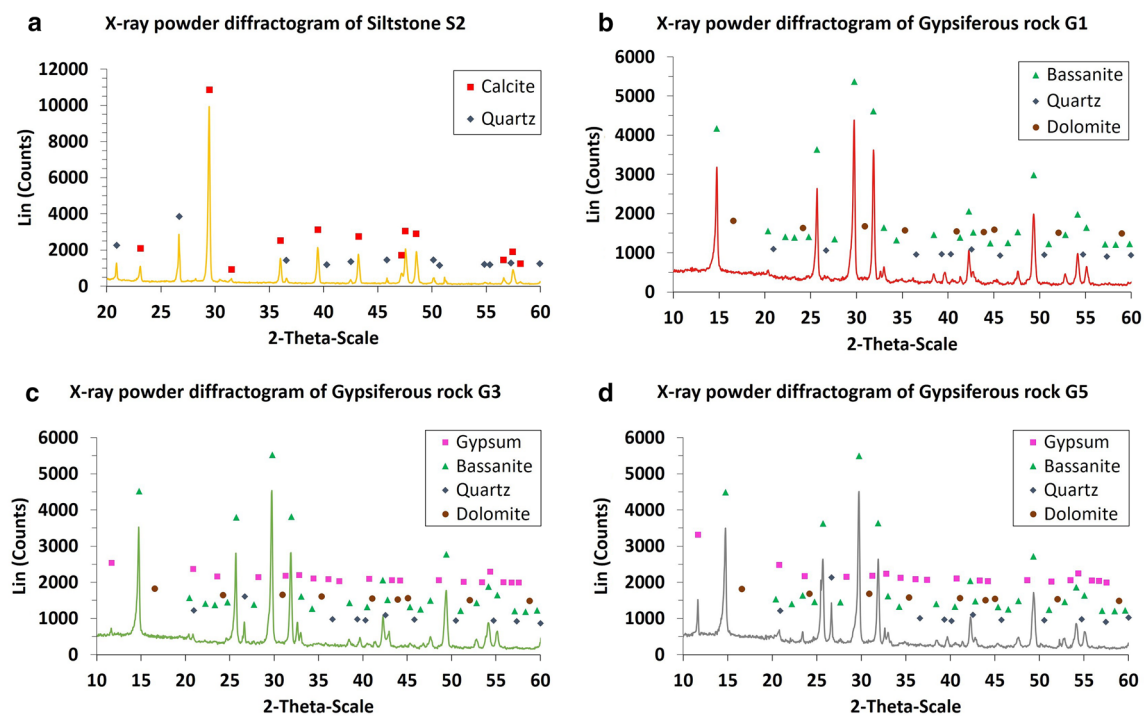
Compound	S2 (%)	G1 (%)	G3 (%)	G5 (%)
Na_2O	0.24	0.41	0.22	–
MgO	0.73	3.84	7.20	3.44
Al_2O_3	0.79	1.78	2.14	2.37
SiO_2	8.13	6.86	8.29	8.42
P_2O_5	–	–	–	0.05
SO_3	0.25	41.51	42.08	36.14
K_2O	0.26	0.27	0.33	0.71
CaO	44.34	32.30	34.85	26.67
TiO_2	0.04	0.13	0.09	0.18
Fe_2O_3	0.56	1.16	1.16	1.07
SrO	0.14	0.35	0.61	0.31
I	–	0.02	–	–
BaO	–	0.21	0.08	0.13
WO_3	0.10	0.15	0.15	0.12
LOI	44.42	11.01	2.79	20.40

Fig. 3 XRD analyses of siltstone (S2) (**a**) and gypsiferous rock (G1, G3 and G5) (**b**, **c** and **d**, respectively)

Fig. 4 Thin-section micro-photographs of siltstone (S2) and gypsiferous rock (G1, G3 and G5) taken with parallel light (**a.1**, **b.1**, **c.1** and **d.1**) and crossed nicols (**a.2**, **b.2**, **c.2** and **d.2**)
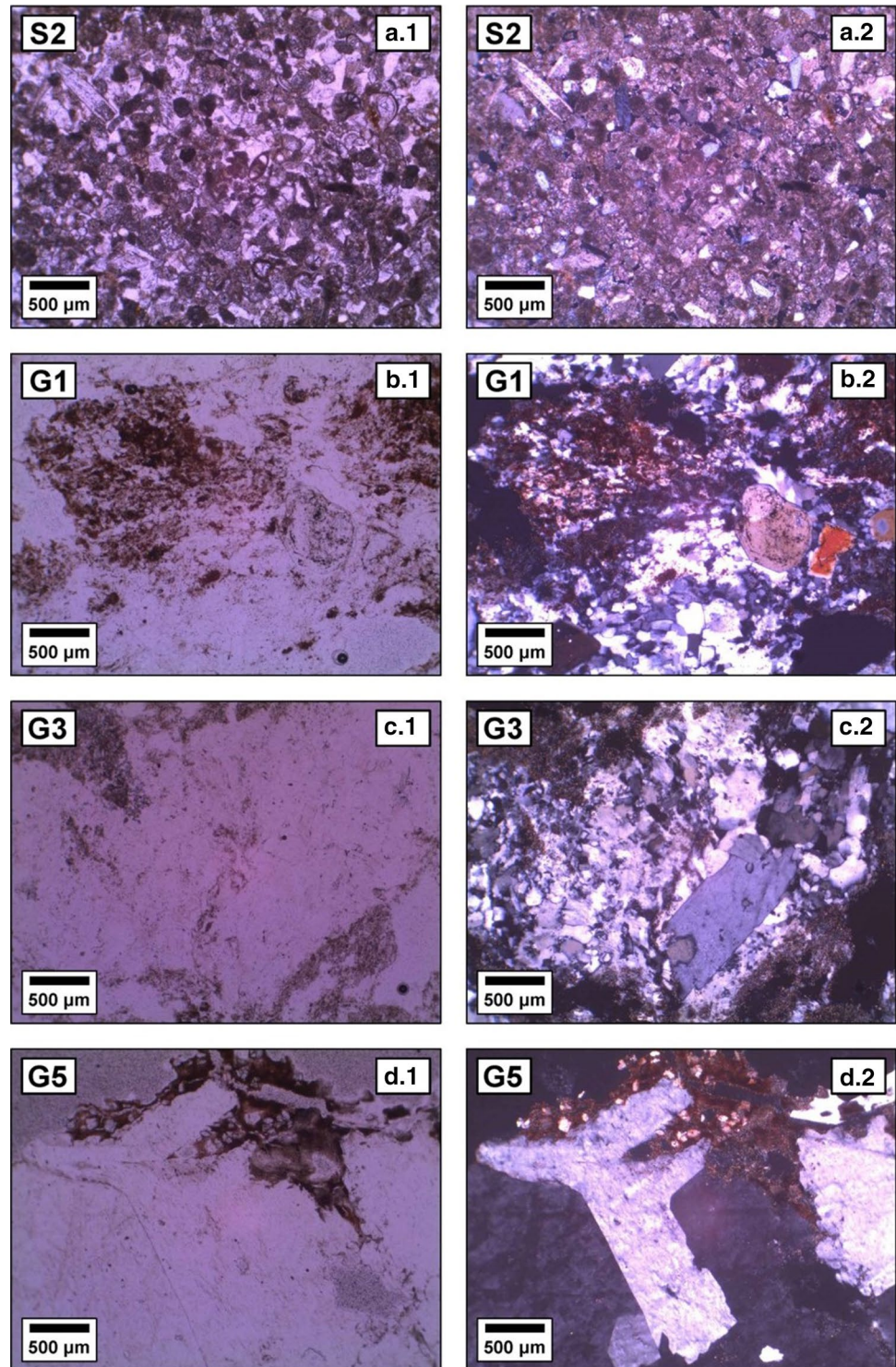
From a petrographic point of view, the siltstone had a grain size of 0.01–0.5 mm, mostly calcite and quartz (monocrystalline and polycrystalline) minerals but also some phyllosilicates (Fig. 4a). As for the gypsiferous rock, factures were filled mainly with laminar microcrystalline gypsum and, to a lesser extent, fibrous gypsum. The gypsum crystals exhibited several morphologies and sizes (50 μm–3 mm) and sometimes showed exfoliation. Also

identified, in addition to bassanite, dolomite and anhydritic and detritic levels formed of monocrystalline and polycrystalline quartz, were calcite crystals and fragments of carbonate rock (Fig. 4b–d).

4.2 Physical Properties

Dry and saturated bulk densities of the siltstone specimens (rock blocks S1 to S4) varied between 1.88 and 1.94 g/cm^3 and 2.19 and 2.23 g/cm^3, respectively, with the highest and lowest bulk density values corresponding to the S3 and S2 specimens, respectively. As for porosity, the S3 specimens had the lowest mean open and total porosity values (26.34 and 26.62%, respectively) and lowest mean water absorption value (13.39%), while the S2 specimens had the highest mean open porosity, total porosity and water absorption values (28.83, 29.29 and 15.11%, respectively). S1 and S4 specimens had mean density and porosity values close to the S2 and S3 specimens, respectively.

As for the gypsiferous rock specimens (rock blocks G1 to G5), all blocks exhibited greater densities and lower porosities than the siltstones and also showed wider ranges because of their greater heterogeneity. Dry and saturated bulk densities varied between 2.03 and 2.23 g/cm^3 and 2.19 and 2.28 g/cm^3, respectively, with the highest and lowest bulk density values corresponding to the G4 and G1 specimens, respectively. G4 specimens also had the lowest mean open and total porosity values (3.22 and 9.32%, respectively) and water absorption value (1.45%), while the G1 specimens had the greatest mean open porosity, total porosity and water absorption values (10.64, 13.72 and 5.12%, respectively). G2 and G3 specimens had similar mean density and porosity values.

The physical properties corresponding to the nine rock blocks, as obtained using traditional techniques, are summarized in Table 4.

Regarding the porous structure of rocks as estimated by means of MIP tests, the siltstones had pore diameters in the range 0.2–60 μm (mainly 0.9–30 μm) and intraparticle and interparticle porosity of around 8 and 22%, respectively (total porosity was close to 30%), while surface area was close to 1.1 m^2/g. The gypsiferous rock showed a wider range of values than the siltstones. Pore diameters were mostly in the interval 1–40 μm, although some specimens had a significant number of pores with diameters of 0.004–0.02 μm. Interparticle and intraparticle porosity values were 2.6–7.7% and 2.2–4.3%, respectively (total porosity was 5.6–12.0%), while surface area, at 2.5 to 3.8 m^2/g, was substantially higher than for the siltstone (Fig. 5).

4.3 Mechanical Properties

According to Agustawijaya (2007), the kind of siltstone and gypsiferous rock studied in this work can be classified as soft (or weak) rock since their UCS values are lower than 20 MPa.

For the siltstone specimens in dry conditions, the highest UCS, $I_{s(50)}$, NPI and E_{st} values − 10.84 MPa, 0.75 MPa, 93 N/mm and 4.94 GPa, respectively—were found for block S3, while the lowest UCS, $I_{s(50)}$, NPI and E_{st} values were found for block S1, with values of 7.70 MPa, 0.43 MPa, 52 N/mm and 2.38 GPa, respectively. These results are consistent with the higher density and lower porosity of the S3 specimens and the lower density and higher porosity of the S1 specimens. As for the other siltstone blocks, S2 (with UCS, $I_{s(50)}$, NPI and E_{st} values of 8.10 MPa, 0.48 MPa, 57 N/mm and 2.84 GPa, respectively) was similar to S1, while S4 (with UCS, $I_{s(50)}$, NPI and E_{st} values of 9.54 MPa, 0.69 MPa, 67 N/mm and 4.91 GPa, respectively) was similar to S3. For the siltstone specimens in saturated conditions, the highest mechanical parameter values were found in S4 followed by S3 while the lowest values were found in S2 followed by S1.

Table 4 Physical properties of the siltstone and gypsiferous rock blocks

Rock block	Physical properties ($\chi \pm \sigma$)				
	ρ_d (g/cm^3)	P_o (%)	ρ_{sat} (g/cm^3)	P (%)	W_a (%)
S1	1.880 ± 0.016	28.45 ± 0.36	2.200 ± 0.007	28.9 1 ± 0.46	14.81 ± 0.27
S2	1.877 ± 0.020	28.83 ± 1.06	2.193 ± 0.020	29.29 ± 1.08	15.11 ± 0.81
S3	1.937 ± 0.039	26.34 ± 1.28	2.227 ± 0.021	26.62 ± 1.34	13.39 ± 0.88
S4	1.933 ± 0.042	26.85 ± 0.82	2.219 ± 0.012	27.31 ± 0.67	13.73 ± 0.56
G1	2.035 ± 0.073	10.64 ± 2.73	2.194 ± 0.025	13.72 ± 2.32	5.12 ± 1.41
G2	2.157 ± 0.038	6.14 ± 1.76	2.268 ± 0.025	9.95 ± 2.19	2.79 ± 0.85
G3	2.148 ± 0.036	7.16 ± 1.16	2.248 ± 0.009	11.30 ± 0.98	3.29 ± 0.56
G4	2.232 ± 0.090	3.22 ± 1.84	2.280 ± 0.021	9.32 ± 2.72	1.45 ± 0.85
G5	2.196 ± 0.073	4.67 ± 2.74	2.248 ± 0.007	10.37 ± 3.03	2.14 ± 1.28

ρ_d, dry density; ρ_{sat}, saturated density; p_o, open porosity; p, total porosity; W_a, water absorption; χ, mean value; σ, standard deviation
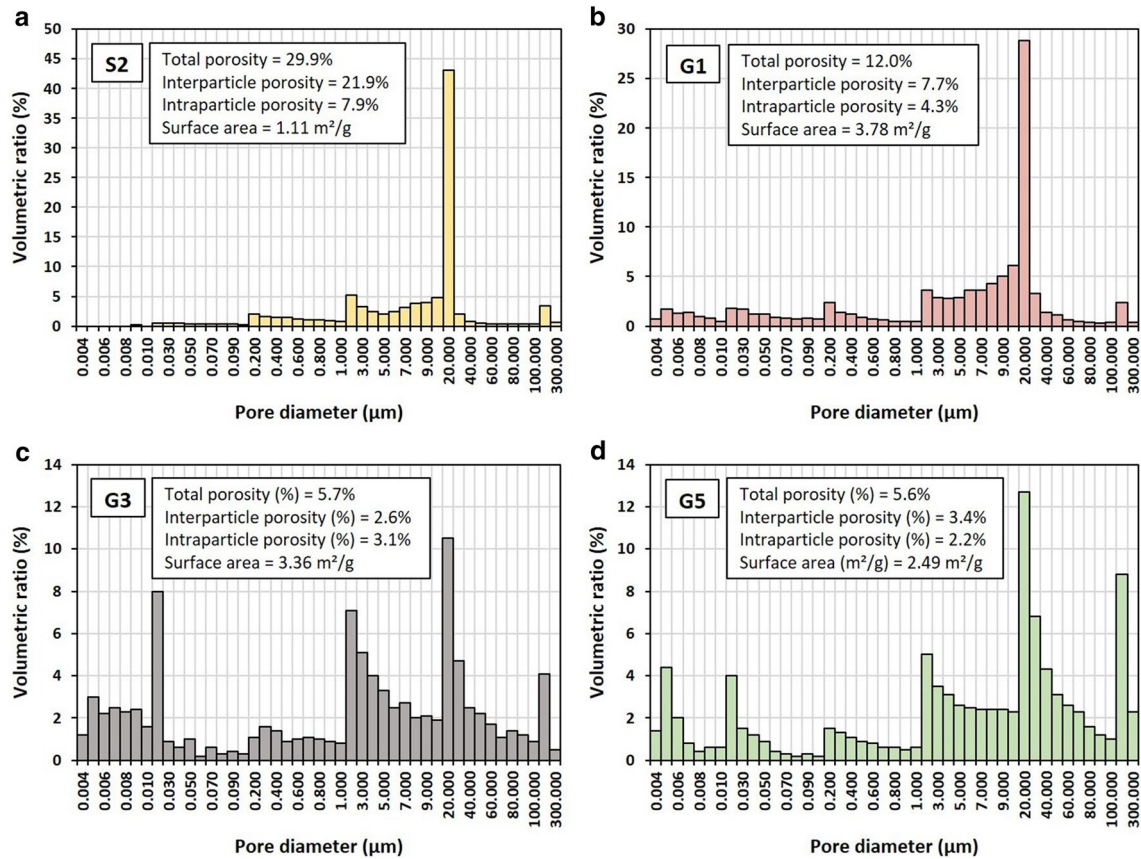
Fig. 5 Variations in volumetric ratios, as measured using mercury intrusion porosimetry, according to pore size distribution in siltstone block S2 (**a**) and gypsiferous blocks G1, G3 and G5 (**b**, **c** and **d**, respectively)

As for gypsiferous rock specimens in dry conditions, the remarkable heterogeneity of this lithology resulted in great variations between specimens from the same gypsiferous rock block. In comparison to the dry siltstone specimens, these specimens had much higher E_{st} values (8.10–20.94 GPa) and slightly higher

Table 5 Unconfined compressive strength (UCS), static Young's modulus (E_{st}), point load strength index ($I_{s(50)}$) and needle penetration index (NPI) values for dry and saturated rock block specimens

Rock block	Mechanical properties ($\chi \pm \sigma$)							
	Dry specimens				Saturated specimens			
	UCS	E_{st}	$I_{s(50)}$	NPI	UCS	E_{st}	$I_{s(50)}$	NPI
	MPa	GPa	MPa	N/mm	MPa	GPa	MPa	N/mm
S1	7.70±0.44	2.38±0.55	0.43±0.18	52±7	2.89±0.76	1.23±0.33	0.24±0.05	25±2
S2	8.10±0.48	2.84±0.63	0.48±0.14	57±8	2.79±0.61	0.91±0.29	0.22±0.06	21±3
S3	10.84±2.14	4.94±1.63	0.75±0.11	93±15	5.14±1.67	1.81±0.92	0.42±0.10	32±5
S4	9.54±2.63	4.91±0.37	0.69±0.24	67±21	5.23±0.66	2.34±0.16	0.46±0.22	32±3
G1	7.67±3.35	10.59±5.55	0.54±0.12	74±12	2.29±1.06	8.45±0.85	0.26±0.06	30±6
G2	8.83±1.47	8.10±1.43	0.42±0.13	59±27	3.28±1.24	4.78±3.52	0.34±0.05	38±19
G3	9.50±0.81	11.19±1.65	0.59±0.12	70±19	2.71±0.76	5.51±3.75	0.39±0.06	22±4
G4	14.47±6.45	20.94±9.63	0.90±0.41	109±3	5.38±3.42	13.29±3.56	0.53±0.47	37±6
G5	12.03±3.97	19.98±12.19	0.83±0.39	91±19	6.89±2.52	15.83±2.89	0.71±0.23	66±35

χ, mean value; σ, standard deviation

UCS (7.67–14.47 MPa), $I_{s(50)}$ (0.42–0.90 MPa) and NPI (59–109 N/mm) values. For gypsiferous rock specimens in saturated conditions, the UCS, $I_{s(50)}$, NPI and E_{st} values were 2.29–6.89 MPa, 0.26–0.71 MPa, 22–66 N/mm and 4.78–15.83 GPa, respectively.

The mechanical properties for the nine rock blocks in dry and saturated conditions are summarized in Table 5.

4.4 NPI, E_{st}, UCS and $I_{s(50)}$ Variations According to Water Saturation

For the siltstone, findings regarding the influence of water saturation indicated a very high drop in NPI values in all specimens when saturated, with the highest decreases occurring in the S2 and S3 specimens (63.9 and 65.8%, respectively), and the lowest reductions measured in the S1 and S4 specimens (51.7 and 52.5%, respectively). Similar changes were observed for the E_{st}, with the highest decreases measured in the S2 and S3 specimens (68.0 and 63.4%, respectively) and the lowest reductions occurring in the S1 and S4 specimens (48.3 and 52.4%, respectively). Regarding UCS, the results showed significant losses; the highest and lowest reductions were found for the S2 and S4 specimens (65.5 and 45.1%, respectively), with intermediate values obtained for the S1 and S3 specimens (62.4 and 52.5%). The order in losses was the same for the $I_{s(50)}$, i.e., 53.6% for S2, 44.9% for S1, 43.2% for S3 and 34.0% for S4.

As for the effect of water saturation on the gypsiferous rock, the findings also pointed to important losses for the NPI (27.0–69.1%), UCS (42.7–71.5%), E_{st} (20.2–50.8%) and $I_{s(50)}$ (14.1–52.3%). The highest and lowest NPI, UCS, and E_{st} reductions were measured for G3 and G5 specimens, respectively. As for $I_{s(50)}$, the highest and lowest values were found for G1 and G5, respectively.

Variations in the mechanical properties measured for all nine rock blocks due to water saturation are plotted in Fig. 6.

For the siltstones, the average reduction in the NPI due to water saturation was very similar to that of the UCS and E_{st}, while the $I_{s(50)}$ reduction was slightly lower. This would suggest that the NPI is an appropriate index to determine the effect of water on siltstone strength and deformability, as it shows greater sensitivity in measuring water content changes than $I_{s(50)}$. While the same conclusion is broadly true for gypsiferous blocks, the greater heterogeneity of this lithology introduces bias in the estimation of the parameters.

In Sects. 4.5 to 4.9 below, to identify significant correlations (P value < 0.05) between paired combinations of NPI, UCS, $I_{s(50)}$ and E_{st} values, we investigate linear, power, exponential and logarithmic curve fits using regression analyses.

4.5 NPI and UCS Correlations

The results of the regression analysis to evaluate UCS and NPI correlations for siltstone and gypsiferous rock pointed to significant power and linear correlation functions. Specifically, the best coefficients of determination (R^2) were obtained for the following through-the-origin linear functions:

For dry and saturated siltstones:

$$\text{UCS} = 0.13389 \cdot \text{NPI} \quad \left(R^2 = 0.9854\right) \tag{17.a}$$

For dry and saturated gypsiferous rocks:

$$\text{UCS} = 0.12559 \cdot \text{NPI} \quad \left(R^2 = 0.9804\right) \tag{17.b}$$

where NPI and UCS are expressed in N/mm and MPa, respectively. Although in our case, the slope of the regression lines was lower than reported in the literature, the functions are quite similar (Fig. 7), indicating that, for siltstone and gypsiferous rock, we obtained higher NPI values (i.e., lower penetration depths) than obtained by other authors for rocks with similar UCS values. Apart from the peculiarities of the tested rocks, this difference of slope could be due to the NPT involves not only the UCS but also at other intrinsic parameters of rock.

4.6 NPI and E_{st} Correlations

The results of the regression analysis to predict values of E_{st} from the NPI for siltstone and gypsiferous rock pointed to significant linear and power functions for both lithologies. The best coefficients of determination were obtained, however, by fitting through-the-origin linear functions, as follows:

For dry and saturated siltstones:

$$E_{st} = 0.05658 \cdot \text{NPI} \quad \left(R^2 = 0.9691\right) \tag{18.a}$$

For dry and saturated gypsiferous rocks:

$$E_{st} = 0.19405 \cdot \text{NPI} \quad \left(R^2 = 0.9422\right) \tag{18.b}$$

where NPI and E_{st} are expressed in N/mm and GPa, respectively. The R^2 value for gypsiferous rock (0.94) was slightly lower than for siltstone (0.97), probably due to the greater differences among the gypsiferous rock specimens than among the siltstone specimens.

For the siltstone, the fitting function was very similar to those proposed by Aydan (2012) and Aydan and Ulusay (2013) for Turkish rocks (Fig. 8), whereas for the gypsiferous rock, we obtained lower NPI values (i.e., greater penetration depths) than obtained by them for rocks with similar E_{st} values.
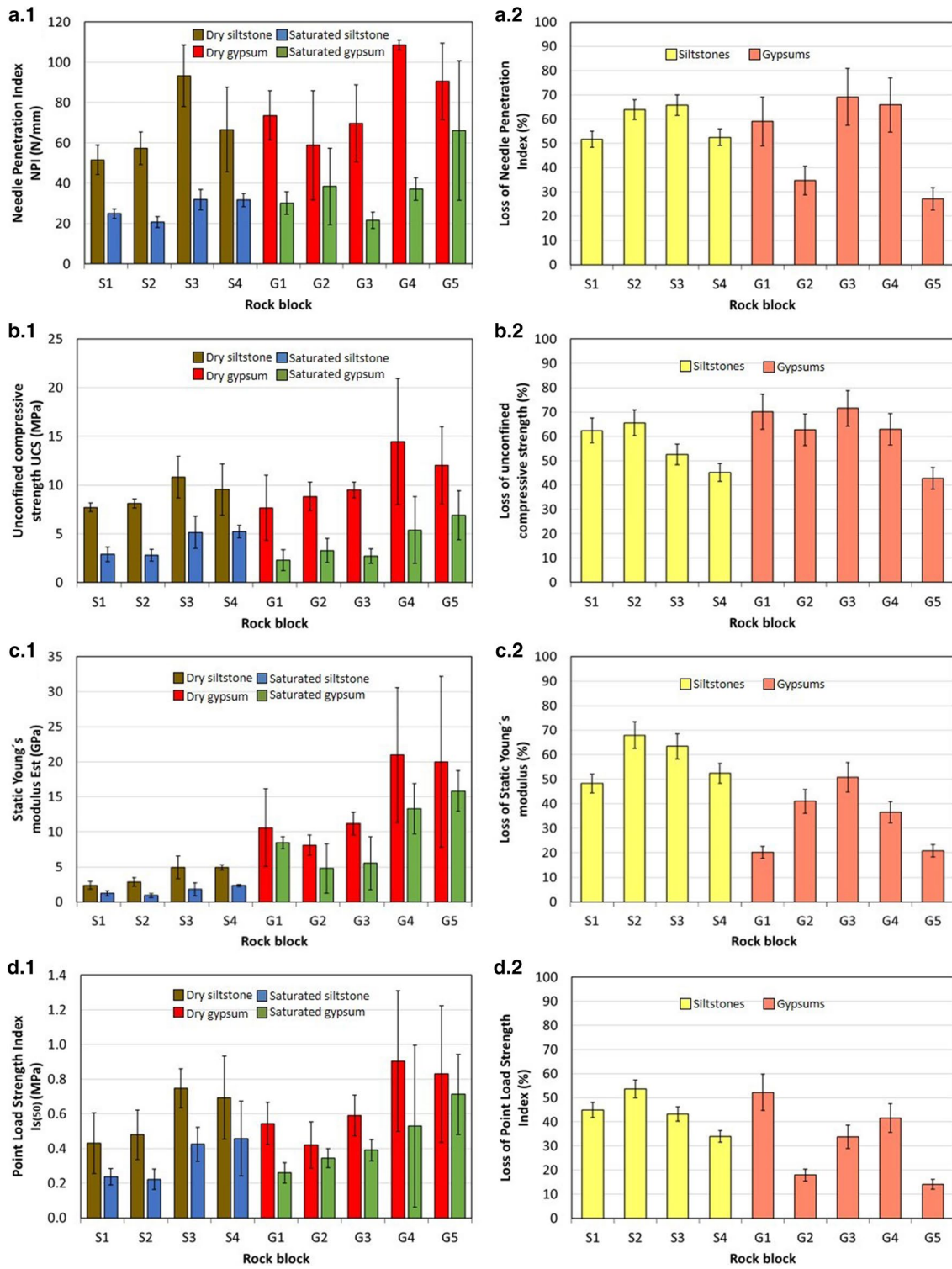
Fig. 6 Influence of water saturation. Left, comparison of values for the needle penetration index (NPI) (**a.1**), unconfined compressive strength (UCS) (**b.1**), static Young's modulus (E_{st}) (**c.1**) and point load strength index ($I_{s(50)}$) (**d.1**) measured for each block in dry and saturated conditions. Right, comparison of percentage changes in NPI (**a.2**), UCS (**b.2**), E_{st} (**c.2**) and $I_{s(50)}$ (**d.2**)

Fig. 7 **a** Needle penetration index (NPI) and unconfined compressive strength (UCS) correlations for dry and saturated siltstone and gypsiferous rock compared to functions reported in published studies. **b** Plotted residuals
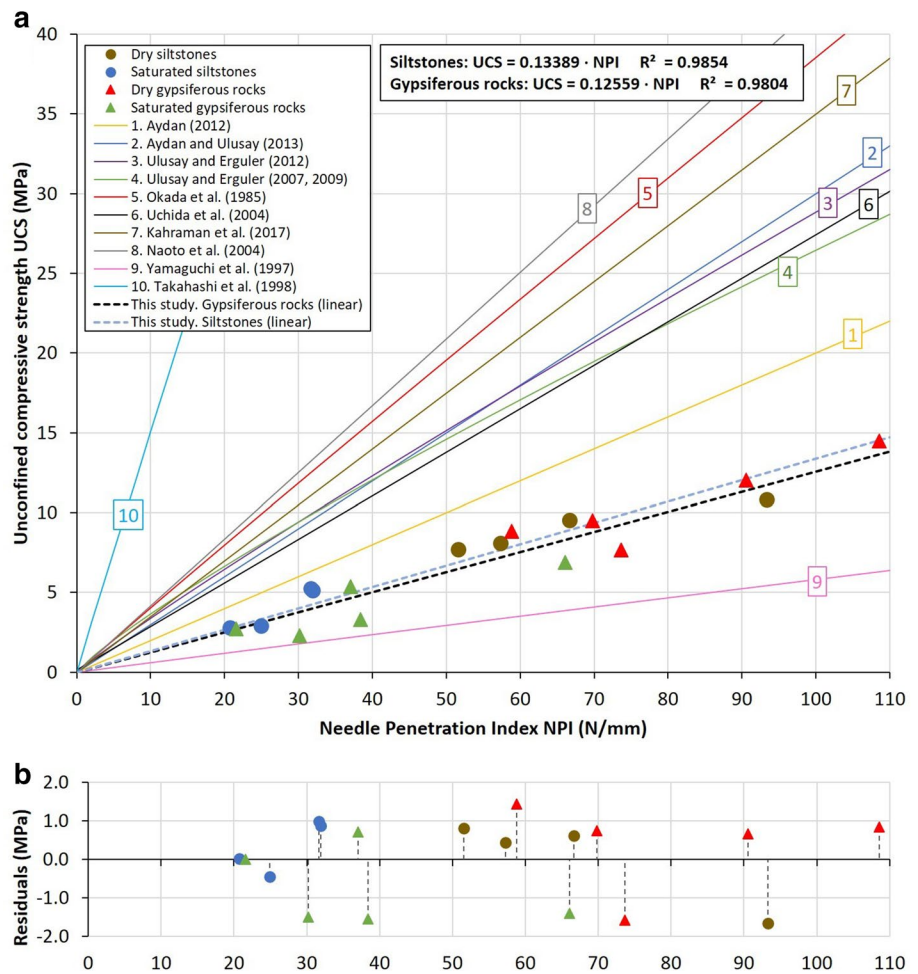
4.7 $I_{s(50)}$ and UCS Correlations

While several authors have proposed linear correlations between $I_{s(50)}$ and UCS for several different rock types, very few studies have focused on soft rocks such as siltstones and gypsiferous rocks. Results for our regression analyses pointed to significant linear and power correlation functions for the $I_{s(50)}$ and UCS for the studied lithologies. In both rock types, the best coefficients of determination were obtained fitting through-the-origin linear functions, as follows:

For dry and saturated siltstones:

$$UCS = 14.2573 \cdot I_{s(50)} \quad \left(R^2 = 0.9825\right) \tag{19.a}$$

For dry and saturated gypsiferous rocks:

$$UCS = 13.6440 \cdot I_{s(50)} \quad \left(R^2 = 0.9433\right) \tag{19.b}$$

where UCS and $I_{s(50)}$ are both expressed in MPa.

Similar values for factor k, which correlates $I_{S(50)}$ and UCS, were reported by Palchik and Hazor (2004) for porous chalks ($k = 8$–18) and by Singh et al. (2012) for several rock types ($k = 14$–16 for softer rocks and $k = 21$–24 for harder rocks)

(Fig. 9). Significant power correlation functions could also be inferred from the data, as reported by Tsiambaos and Sabatakakis (2004), Kahraman (2014), Diamantis et al. (2009) and Tziallas et al. (2009) for Greek and Turkish rocks, although the coefficients of determination would be lower. The discrepancies between linear regression models and test data on UCS and $I_{s(50)}$ observed in the residual plot could be attributed to the slight differences between some rock blocks and others, as well, to the different failure mode of specimens in the UCS test. In this line, although the vast majority of specimens fail by axial splitting, very few of them fail by shear macrofracture.

4.8 $I_{s(50)}$ and E_{st} Correlations

Results for our regression analyses pointed to significant power and linear correlations between $I_{s(50)}$ and E_{st} for both lithologies, with the best coefficients of determination obtained with through-the-origin linear functions, as follows:

For dry and saturated siltstones:

Fig. 8 **a** Needle penetration index (NPI) and static Young's modulus (E_{st}) correlations for dry and saturated siltstone and gypsiferous rock compared to functions reported in published studies. **b** Plotted residuals
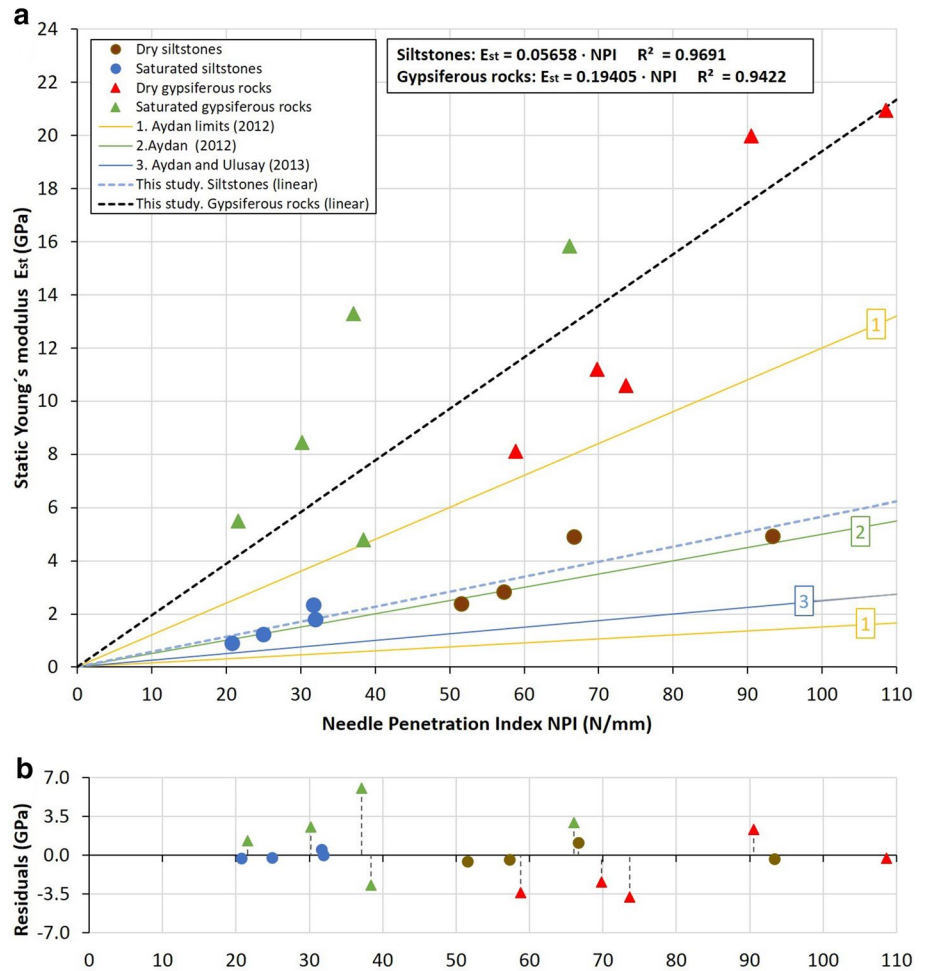
$$E_{st} = 6.05674 \cdot I_{s(50)} \quad (R^2 = 0.9763) \tag{20.a}$$

For dry and saturated gypsiferous rocks:

$$E_{st} = 21.89103 \cdot I_{s(50)} \quad (R^2 = 0.9775) \tag{20.b}$$

where E_{st} and $I_{s(50)}$ are expressed in GPa and MPa, respectively.

Similar findings were reported by Daoud et al. (2017) and can be inferred from Kurtulus et al. (2012) (Fig. 10). Our results confirm that both the NPT and PLT can be used to indirectly estimate UCS and E_{st} for dry and saturated siltstone and gypsiferous rock. However, note that, since it is a destructive test, the PLT cannot be used for protected buildings or to monitor rock structures.

4.9 NPI and $I_{s(50)}$ Correlations

Although both the NPT and $I_{s(50)}$ have been used for indirect estimation of UCS, no correlations between them have been published in the literature. In our regression analysis, we found that significant linear and power correlation functions

could be established between these parameters for siltstone and gypsiferous rock (as might be expected given the results reported above). The best fits were obtained with power-law type regressions (Fig. 11), as follows:

For dry and saturated siltstones:

$$I_{s(50)} = 0.0248 \cdot NPI^{0.7611} \quad (R^2 = 0.8303) \tag{21.a}$$

For dry and saturated gypsiferous rocks:

$$I_{s(50)} = 0.0417 \cdot NPI^{0.6328} \quad (R^2 = 0.6764) \tag{21.b}$$

where NPI and $I_{s(50)}$ are expressed in N/mm and MPa, respectively.

5 Discussion

This paper explores the potential of the NPT and the PLT for indirectly estimating UCS and E_{st} for siltstones and gypsiferous soft rocks widely present in southeastern Spain in dry and saturated states. The siltstone is a low-density and very porous rock, with small UCS and E_{st} values. The gypsiferous

Fig. 9 **a** Point load strength index ($I_{s(50)}$) and unconfined compressive strength (UCS) correlations for dry and saturated siltstone and gypsiferous rock compared to functions reported in published studies. **b** Plotted residuals
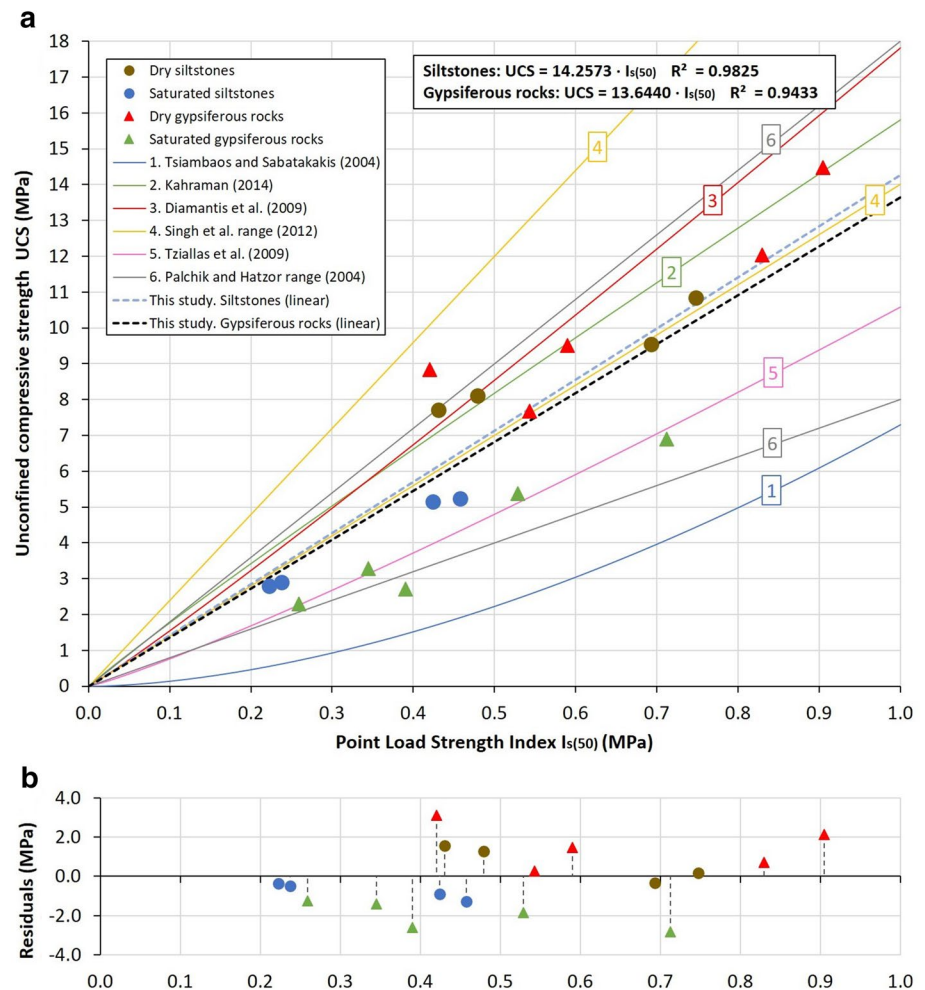

rock has smaller porosity and higher density, similar UCS value and a higher E_{st} value. Furthermore, both rock types exhibited a marked water weakening effect. Specifically, we obtained a UCS reduction of $56.4 \pm 8.1\%$ in the siltstone and of $62.0 \pm 10.3\%$ in the gypsiferous rock and an E_{st} reduction of $58.0 \pm 7.9\%$ in the siltstone and of $33.9 \pm 11.9\%$ in the gypsiferous rock. These results are similar to those previously reported by Erguler and Ulusay (2009) and Yilmaz (2010).

One important finding of this study is that it is possible to estimate mechanical property changes induced by water saturation from reductions in the NPI and $I_{(s50)}$ values, which means that relatively more cost-effective and rapid tests like the PLT and NPT can be used. However, the NPT was more sensitive than the PLT in evaluating the saturation effects on rock strength in both types of rock; NPI reductions were $58.4 \pm 6.4\%$ for the siltstone and $51.1 \pm 17.0\%$ for the gypsiferous rock, while the $I_{s(50)}$ reductions were more moderate, at $43.9 \pm 7.0\%$ for the siltstone and $31.9 \pm 14.3\%$ for the gypsiferous rock. This greater water sensitivity of the NPT means that it can be used in rocks where water effects

are less intense, i.e., in a variety of soft or very soft rocks. However, the PLT has the advantage that it can be used in a wider range of rocks overall where the use of the NPT would not be possible due to negligible needle penetration in harder rock types.

The UCS, E_{st}, NPI and $I_{s(50)}$ reductions can be attributed to different and possibly simultaneously occurring physical, chemical and mineralogical causes. One cause could be the decreased surface energy of crack edges when a pore is full of water (Ballivy and Colin 1999); i.e., the moisture diminishes the spread of free surface energy, thereby facilitating micro-crack propagation by reducing UCS and E_{st} values (Vasarhelyi and Ledniczky 1999). Another cause could be the weakening of cementation between grains through dissolution or dispersion (chemical and corrosive deterioration); the presence of water could induce structural changes such as reduced cement quality, lost grain-to-grain contact area, dissolution of calcite or other minerals in the rock matrix or weakened intergranular bonds. All these effects increase the porosity of a rock and consequently reduces its strength. Yet another cause, which could lead to a weakening

Fig. 10 **a** Point load strength index ($I_{s(50)}$) and static Young's modulus (E_{st}) correlations for dry and saturated siltstone and gypsiferous rock compared to functions reported in published studies. **b** Plotted residuals
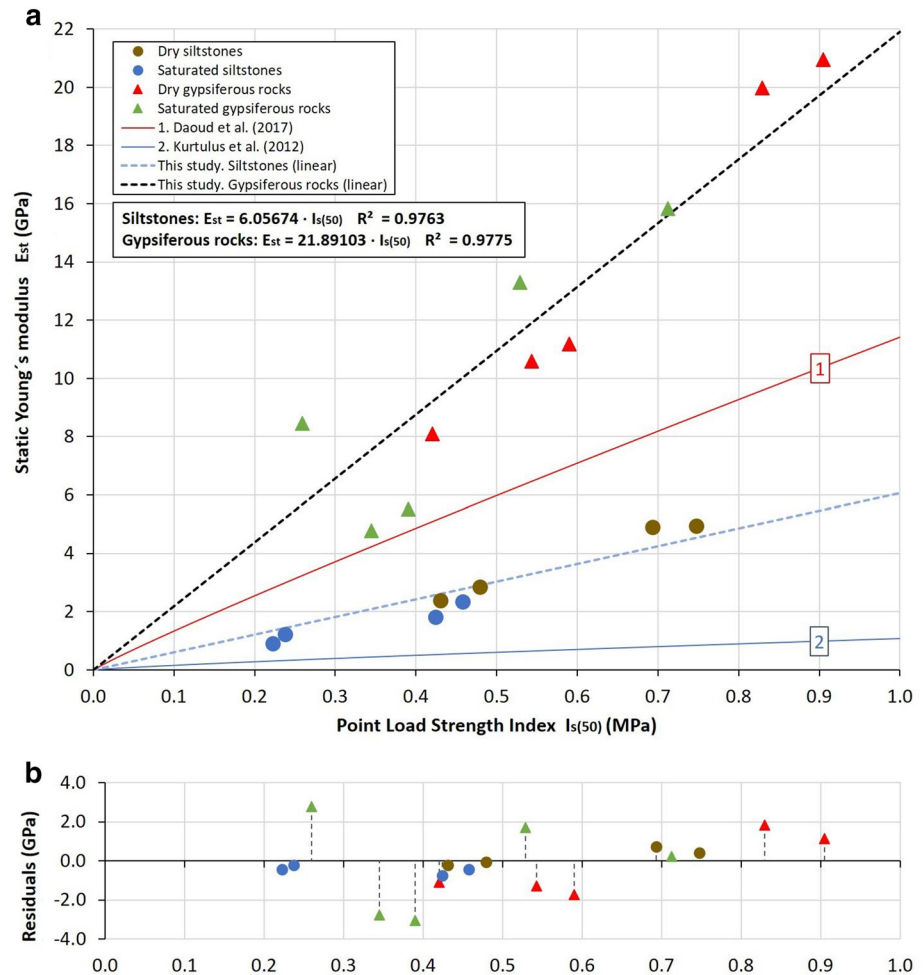
of mechanical properties, is the swelling of clay minerals, which is very pertinent to clay-bearing sandstones or argillaceous rocks (Erguler and Ulusay 2009; Tiennot et al. 2019). In this sense, it is important to note that siltstones have small amounts of phyllosilicates and that gypsiferous rocks also contain only very small quantities of clay. The water-weakening mechanism takes place in three stages: the water first penetrates the rock through micro-sized discontinuities, then induces volumetric swelling of clay minerals and the dissolution of carbonate, and, finally, those two effects propagate and connect up cracks (Wong et al. 2016). Finally, an additional factor explaining the weakening of mechanical properties in gypsiferous rocks could be the expansive transformation of bassanite into gypsum due to hydration during the saturation process (Van Driessche et al. 2012).

Another important result of this study is the proposal of significant linear correlation functions not only between the NPI and the UCS but also between the NPI and the E_{st} for both types of rocks and valid for both dry and saturated conditions. These correlations are especially good (i.e., they present a high R^2) and significant (i.e., P value < 0.05) for siltstone compared to gypsiferous rock, due to the greater

homogeneity of the former, and allow indirect evaluation of the uniaxial strength and deformability of soft rocks using the NPT—a relatively inexpensive and rapid test that does not require any special preparation of the specimens. Furthermore, the NPT can be considered a non-destructive test as it causes practically negligible damage to the rock surface. For this reason, it could feasibly be used to evaluate the mechanical properties of protected natural rock structures and historical or heritage stone buildings. As for the PLT, given the existence of significant correlations between the $I_{s(50)}$ and UCS and between the $I_{s(50)}$ and E_{st}, it could be used as a complementary method to the NPT and could be especially useful to estimate the strength and deformability of somewhat harder rocks for which the NPT is not feasible.

Additionally, the significant correlations between the NPI and the $I_{s(50)}$ suggest the use of the NPT to estimate the strength of soft rocks against concentrated or point loads in a non-destructive manner, something which would not be possible with the PLT. Furthermore, given that the Schmidt hammer test is not suitable for soft rocks (Aydin 2009) and is less sensitive to mechanical property changes, the NPT may be the only viable non-destructive way to estimate UCS,

Fig. 11 **a** Point load strength index ($I_{s(50)}$) and needle penetration index (NPI) correlations for dry and saturated siltstone and gypsiferous rock. **b** Plotted residuals
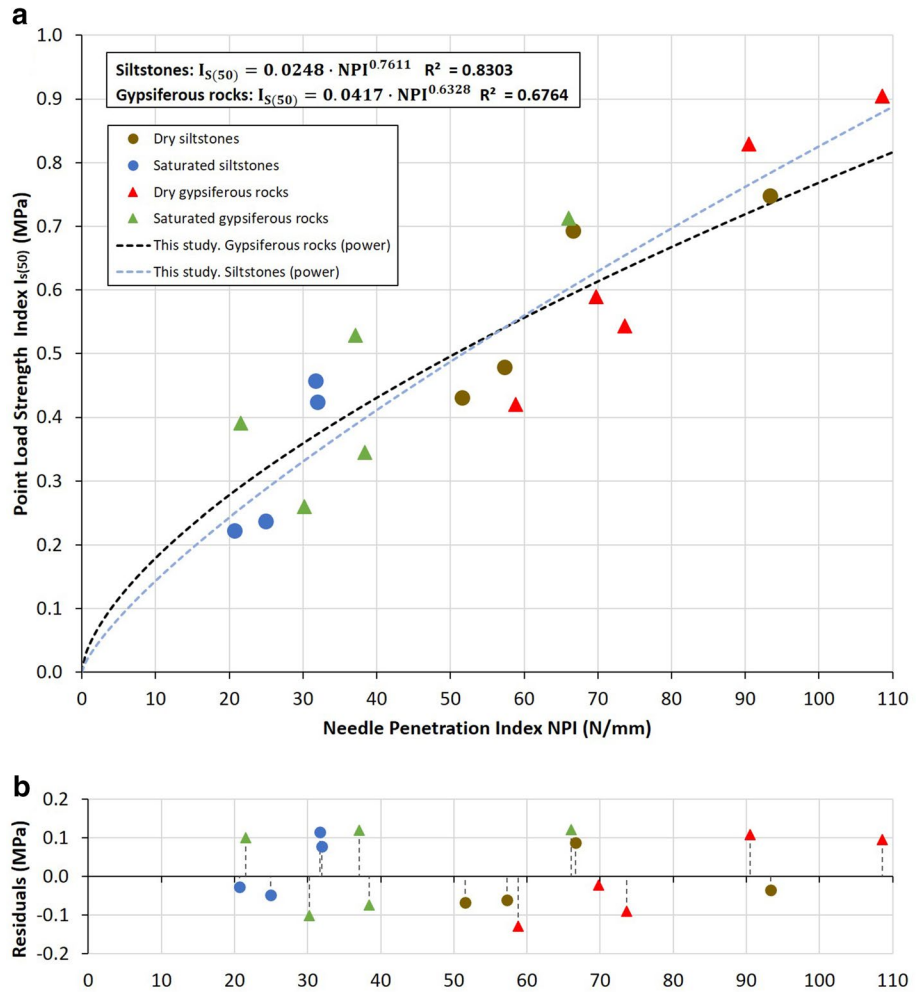
Table 6 Comparative characteristics of tests used to determine unconfined compressive strength (UCS) in rock

Test	UCS	Schmidt hammer test	Point load test	Needle penetration test
Range of application for UCS determination (MPa)	Unlimited	10–400	1–250	< 20
Determination of UCS	Direct	Indirect	Indirect	Indirect
Determination of E_{st}	Direct	Not suitable	Indirect	Indirect
Application	LAB	FLD/LAB	FLD/LAB	FLD/LAB
Specimen preparation requirements	Yes (*)	No	No	No
Destructive test type	Yes	No	Yes	No
Suitable for soft rock	Yes	No (**)	Yes	Yes
Relative cost	High	Low	Low	Low
Sensitivity	Medium	Very low	Low	High
Test duration (***)	Long	Very short (****)	Short (****)	Very short (****)
Time to results calculation	Short	Very short	Long	Short

FLD: Field; LAB: Laboratory

(*) Some difficulties in preparing soft rocks specimens

(**) Difficulties of application to soft rocks due to the required high energy

(***) Including time required for specimen preparation

(****) This time can be "long" when testing using regular (cylindrical) specimens

$I_{s(50)}$ and E_{st} values, as particularly important input data for a large number of rock engineering applications, including rock mass characterization using classification systems such as RMR. Another advantage of the NPT is that test performance and results retrieval are faster than for the PLT, an important issue, for instance, for tunnels where decisions on supports need to be almost immediate.

A comparative analysis of the different tests available to obtain the mechanical properties of soft rocks, as based on our experience and the results of this study, is provided in Table 6. The most important advantages of NPT are: (a) it is particularly suited for the characterization of soft rocks (with UCS lower than 20 MPa) and is highly sensitive to UCS changes; (b) it does not require either special specimen preparations or heavy expensive equipment; (c) it can be used in both the field and in the laboratory; (d) it requires little to no time for testing and results calculation, which is very useful for determining strength properties in particular circumstances (e.g., for tunnels); and (e) because it is non-destructive, rock mechanical strength can be estimated without destroying or rendering protected natural structures or historical or heritage buildings.

6 Conclusions

In terms of the potential of the NPT and PLT for indirectly estimating UCS and E_{st} for siltstone and gypsiferous rock in dry and saturated states, our main conclusions are as follows:

1. The NPT is a non-destructive, inexpensive, simple and rapid method that can be used in dry and saturated soft rocks to indirectly estimate strength and deformability, in accordance with our proposed linear correlations between the NPI and UCS and between the NPI and E_{st} for both lithologies.
2. The NPI is a suitable index to estimate the influence of water on strength and deformability of soft rocks, given that losses due to water saturation are similar to those for UCS and E_{st}.
3. The NPT can be considered non-destructive, given that the damage to rock specimens caused by needle penetration is negligible. This fact, together with the correlations between the NPI and mechanical properties, means that the NPT is especially suitable for estimating strength and deformability parameters for natural or artificial historical rock structures and heritage and protected ancient monuments as well as for monitoring and restoring stone constructions.
4. The PLT, while it can also be used to indirectly estimate UCS and E_{st} for both lithologies, is a destructive test and is also less sensitive in measuring changes in rock

properties caused by water. This limits its potential for use for stone that must be preserved and for less water-sensitive rocks.
5. Finally, the good correlation between NPI and $I_{s(50)}$ indicates the possibility of using the NPT to estimate the strength of soft rocks against concentrated or point loads in a non-destructive and rapid way.

References

AENOR (1990a) UNE 22-950-90-1. Propiedades mecánicas de las rocas. Ensayos para la determinación de la resistencia. Parte 1: Resistencia a la compresión uniaxial. Asociación Española de Normalización y Certificación, Madrid, pp 1–4

AENOR (1990b) 'UNE 22-950-90-3. Propiedades mecánicas de las rocas. Ensayos para la determinación de la resistencia. Parte 3: Determinación del módulo de elasticidad (Young) y del coeficiente de Poisson. Asociación Española de Normalización y Certificación, Madrid

AENOR (1993) UNE 103-200-93. Determinación del contenido de carbonatos en los suelos. Asociación Española de Normalización y Certificación, Madrid

AENOR (1994) UNE 103-302-94. Determinación de la densidad relativa de las partículas de un suelo. Asociación Española de Normalización y Certificación, Madrid, p 4. https://es.scribd.com/document/269476259/UNE-103-302-94

AENOR (2007) UNE-EN 1936. Métodos de ensayo para piedra natural. Determinación de la densidad real y aparente y de la porosidad abierta y total. Asociación Española de Normalización y Certificación, Madrid

AENOR (2008) UNE-EN 13755. Métodos de ensayo para piedra natural. Determinación de la absorción de agua a presión atmosférica. Asociación Española de Normalización y Certificación, Madrid, pp 1–10

Agustawijaya DS (2007) The uniaxial compressive strength of soft rock. Civil Eng Dimens 9(1):9–14

Al-Jassar SH, Hawkins AB (1979) Geotechnical properties of the carboniferous limestone of the Bristol area. The influence of petrography and chemistry. In: International society for rock mechanics and rock engineering (ed) 4th ISRM congress, Montreux, pp 2–8

Aydan Ö (2012) The inference of physico-mechanical properties of soft rocks and the evaluation of the effect of water content and weathering on their mechanical properties from needle penetration tests. In: 46th US rock mechanics/geomechanics symposium, vol 1, pp 410–415

Aydan Ö, Ulusay R (2013) Geomechanical evaluation of derinkuyu antique underground city and its implications in geoengineering. Rock Mech Rock Eng 46(4):731–754. https://doi.org/10.1007/s00603-012-0301-7

Aydin A (2009) ISRM suggested method for determination of the Schmidt hammer rebound hardness. Int J Rock Mech Min Sci 46(3):627–634. https://doi.org/10.1016/j.ijrmms.2008.01.020

Ballivy G, Colin JC (1999) Stockage souterrain: influence de la nature du fluide sur les propriétés mécaniques de la roche en paroi. In: 9th International congress on rock mechanics, pp 563–567

Bieniawski Z (1975) The point load test in geotechnical practice. Eng Geol 9(1):1–11

Broch E, Franklin JA (1972) The point-load strength test. Int J Rock Mech Min Sci 9(6):669–676. https://doi.org/10.1016/0148-9062(72)90030-7

Carter P, Sneddon M (1977) Comparison of Schmidt Hammer, point load and unconfined compression tests in carboniferous strata. In: Castle U (ed) Proceeding of a conference on rock engineering, Tyne, England, pp 197–210

Daoud HSD, Rashed KAR, Alshkane YMA (2017) Correlations of uniaxial compressive strength and modulus of elasticity with point load strength index, pulse velocity and dry density of limestone and sandstone rocks in Sulaimani Governorate, Kurdistan Region, Iraq. J Zankoy Sulaimani Part A (Pure Appl Sci) 19(3&4):57–72. https://doi.org/10.17656/jzs.10632

Das B (1985) Evaluation of the point load strength for soft rock classification. In: Proceeding of the 4th international conference on ground control in mining, Morgantown, pp 220–226

Diamantis K, Gartzos E, Migiros G (2009) 'Study on uniaxial compressive strength, point load strength index, dynamic and physical properties of serpentinites from Central Greece: test results and empirical relations. Eng Geol 108(3–4):199–207. https://doi.org/10.1016/j.enggeo.2009.07.002

E1621-13, A (2013) Standard guide for elemental analysis by wavelength dispersive X-ray fluorescence spectrometry. ASTM International, West Conshohocken

Erguler ZA, Ulusay R (2009) Water-induced variations in mechanical properties of clay-bearing rocks. Int J Rock Mech Min Sci 46(2):355–370. https://doi.org/10.1016/j.ijrmms.2008.07.002

Franklin JA (1985) Suggested method for determining point load strength. Int J Rock Mech Min Sci. https://doi.org/10.1016/0148-9062(85)92327-7

Hawkins AB (1998) Aspects of rock strength. Bull Eng Geol Env 57(1):17–30. https://doi.org/10.1007/s100640050017

Ichise Y, Yamakado A, Takano S (1974) High pressure jet-grouting method. US Patent 3,802,203

ISRM (1977) Suggested methods for determining the uniaxial compressive strength and deformability of rock materials. International Society for Rock Mechanics, pp 0–3

Jermy C, Bell F (1991) Coal bearing strata and the stability of coal mines in South Africa. In: Engineering, I. S. for R. M. and R. (ed) 7th ISRM congress, Aachen, pp 1125–1131

Kahraman S (2014) The determination of uniaxial compressive strength from point load strength for pyroclastic rocks. Eng Geol. https://doi.org/10.1016/j.enggeo.2013.12.009

Kahraman S, Gunaydin O (2008) Indentation hardness test to estimate the sawability of carbonate rocks. Bull Eng Geol Environ 67(4):507–511. https://doi.org/10.1007/s10064-008-0162-1

Kahraman S, Fener M, Kozman E (2012) Predicting the compressive and tensile strength of rocks from indentation hardness index. J South Afr Inst Min Metall 112(5):331–339

Kahraman S et al (2017) The needle penetration test for predicting coal strength. J South Afr Inst Min Metall 117(6):587–591. https://doi.org/10.17159/2411-9717/2017/v117n6a9

Kohno M, Maeda H (2012) Relationship between point load strength and uniaxial compressive strength of hydrothermally altered soft rocks. Int J Rock Mech Min Sci 50:147–157. https://doi.org/10.1201/b11646-121

Kurtulus C, Bozkurt A, Endes H (2012) Physical and mechanical properties of serpentinized ultrabasic rocks in NW Turkey. Pure Appl Geophys 169(7):1205–1215. https://doi.org/10.1007/s00024-011-0394-z

Li D, Wong LNY (2013) Point load test on meta-sedimentary rocks and correlation to UCS and BTS. Rock Mech Rock Eng 46(4):889–896. https://doi.org/10.1007/s00603-012-0299-x

Li Z et al (2016) Applicability of needle penetration test on soft rocks. Electron J Geotech Eng 21(23):7209–7222

Maruto Co. Ltd. (2006) Penetrometer for soft rock: model SH-70 instruction manual, Tokyo

Naoto U, Yoshitake E, Hidehiro O, Norihiko M (2004) Strength evaluation of deep mixing soil-cement by needle penetration test. J Jpn Soc Soil Mech Found Eng 52(7):23–25

Okada S, Izumiya Y, Iizuka Y, Horiuchi S (1985) The estimation of soft rock strength around a tunnel by needle penetration test. J Jpn Soc Soil Mech Found Eng 33(2):35–38

Palchik V, Hatzor YH (2004) The influence of porosity on tensile and compressive strength of porous chalks. Rock Mech Rock Eng 37(4):331–341. https://doi.org/10.1007/s00603-003-0020-1

Read JRL, Thornten PN, Regan WM (1980) A rational approach to the point load test. In: 3rd Australian-New Zealand geomechanics conference, Wellington, pp 35–39

Rusnak J, Mark C (2000) Using the point load test to determine the uniaxial compressive strength of coal measure rock. In: Peng SS, Mark C (eds) Proceedings of the 19th international conference on ground control in mining, Morgantown, West Virginia, pp 362–371

Sabatakakis N et al (2008) Index properties and strength variation controlled by microstructure for sedimentary rocks. Eng Geol 97(1–2):80–90. https://doi.org/10.1016/j.enggeo.2007.12.004

Sadeghiamirshahidi M, Vitton SJ (2019) Mechanical properties of Michigan Basin's gypsum before and after saturation. J Rock Mech Geotech Eng 11(4):739–748. https://doi.org/10.1016/j.jrmge.2018.10.006

Singh TN, Kainthola A, Venkatesh A (2012) Correlation between point load index and uniaxial compressive strength for different rock types. Rock Mech Rock Eng 45(2):259–264. https://doi.org/10.1007/s00603-011-0192-z

Smith HJ (1997) The point load test for weak rock in dredging applications. Int J Rock Mech Min Sci 34:295

Szwedzicki T (1998) Draft ISRM suggested method for determining the indentation hardness index of rock materials. Int J Rock Mech Min Sci 6:833–835

Takahashi K, Noto K, Yokokawa I (1998) Strength characteristics of Kobe Formation in Akashi Strata. In: 10th Japan national conference on geotechnical engineering. The Japanese Geotechnical Society, pp 1231–1232

Tiennot M, Mertz JD, Bourgès A (2019) Influence of clay minerals nature on the hydromechanical and fracture behaviour of stones. Rock Mech Rock Eng 52(6):1599–1611. https://doi.org/10.1007/s00603-018-1672-1

Tiryaki B, Bolukbasi N (2007) A model for practical estimation of rock cuttability using cone indenter test. In: 1st Mining machinery symposium of Turkey, pp 1–7. https://doi.org/10.13140/2.1.3185.0569

Tsiambaos G, Sabatakakis N (2004) Considerations on strength of intact sedimentary rocks. Eng Geol 72(3–4):261–273. https://doi.org/10.1016/j.enggeo.2003.10.001

Tziallas GP, Tsiambaos G, Saroglou H (2009) Determination of rock strength and deformability of intact rocks. Electron J Geotech Eng 14:1–12

Ulusay R, Erguler ZA (2012) Needle penetration test: evaluation of its performance and possible uses in predicting strength of weak and soft rocks. Eng Geol. https://doi.org/10.1016/j.enggeo.2012.08.007

Ulusay R et al (2014) ISRM suggested method for the needle penetration test. Rock Mech Rock Eng 47(3):1073–1085. https://doi.org/10.1007/s00603-013-0534-0

Vallejo L, Walsh R, Robinson M (1989) Correlation Between unconfined compressive and point load strength for appalachian rocks. In: Proceeding of the 30th U.S. symposium on rock mechanics, pp 461–468

Van Driessche AES et al (2012) The role and implications of bassanite as a stable precursor phase to gypsum precipitation. Science 336:69–72. https://doi.org/10.1126/science.1215648

Vasarhelyi B, Ledniczky K (1999) Influence of water-saturation and weathering on mechanical properties of Sivac marble. In: 9th International congress on rock mechanics, pp 691–693

Wong LNY, Maruvanchery V, Liu G (2016) Water effects on rock strength and stiffness degradation. Acta Geotech 11(4):713–737. https://doi.org/10.1007/s11440-015-0407-7

Yamaguchi Y, Ogawa N, Kawasaki M, Nakamura A (1997) Evaluation of seepage failure resistance potential of dam foundation with simplified tests. J Jpn Soc Eng Geol 38(3):130–144

Yilmaz I (2010) Influence of water content on the strength and deformability of gypsum. Int J Rock Mech Min Sci 47(2):342–347. https://doi.org/10.1016/j.ijrmms.2009.09.002